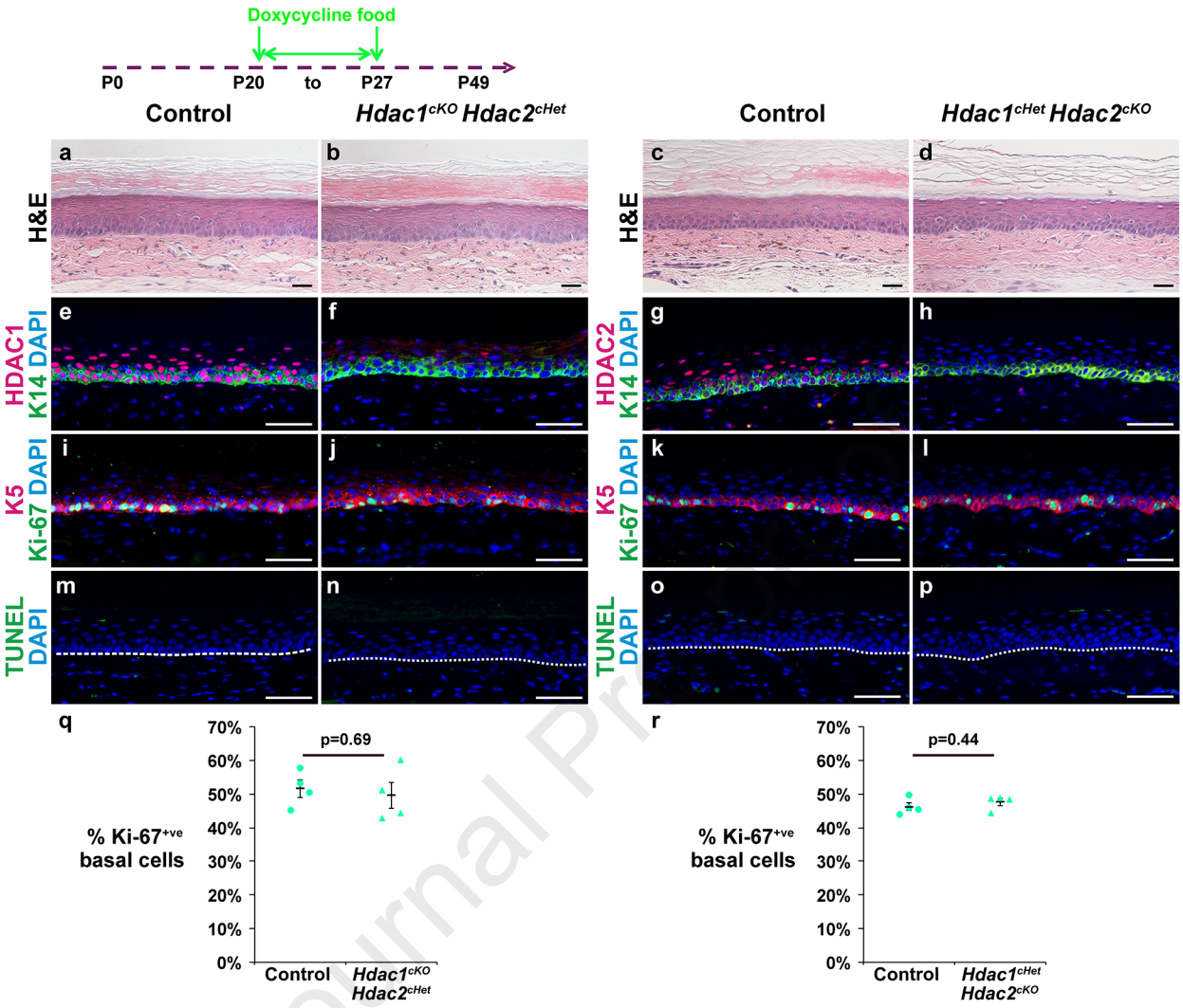
Doxycycline food
P0
P20
to
P27
P49
Control
Hdac1cKO Hdac2cHet
Control
Hdac1cHet Hdac2cKO
a
b
c
d
H&E
e
f
g
h
HDAC1 K14 DAPI
HDAC2 K14 DAPI
i
j
k
l
K5 Ki-67 DAPI
m
n
o
p
TUNEL DAPI
q
r
p=0.69
p=0.44
% Ki-67+ve basal cells
70%
60%
50%
40%
30%
20%
10%
0%
Control
Hdac1cKO Hdac2cHet
Hdac1cHet Hdac2cKO

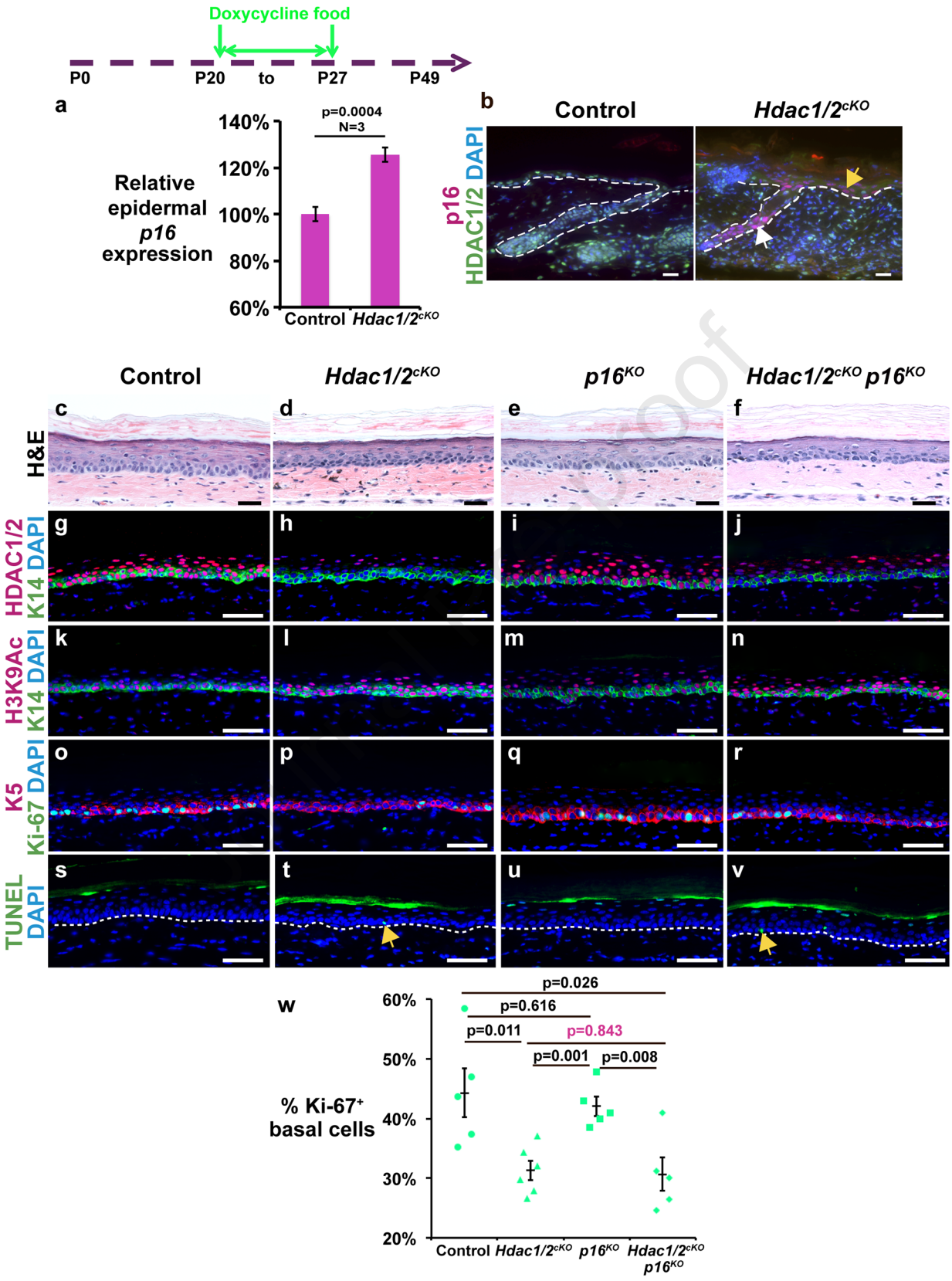
Doxycycline food
P0
P20
to
P27
P49
a
Relative epidermal p16 expression
p=0.0004
N=3
140%
120%
100%
80%
60%
Control
Hdac1/2cKO
b
Control
Hdac1/2cKO
p16
HDAC1/2 DAPI
Control
Hdac1/2cKO
p16KO
Hdac1/2cKO p16KO
H&E
HDAC1/2 K14 DAPI
H3K9Ac K14 DAPI
K5 Ki-67 DAPI
TUNEL DAPI
w
% Ki-67+ basal cells
p=0.026
p=0.616
p=0.011
p=0.843
p=0.001
p=0.008
60%
50%
40%
30%
20%
Control
Hdac1/2cKO
p16KO
Hdac1/2cKO p16KO

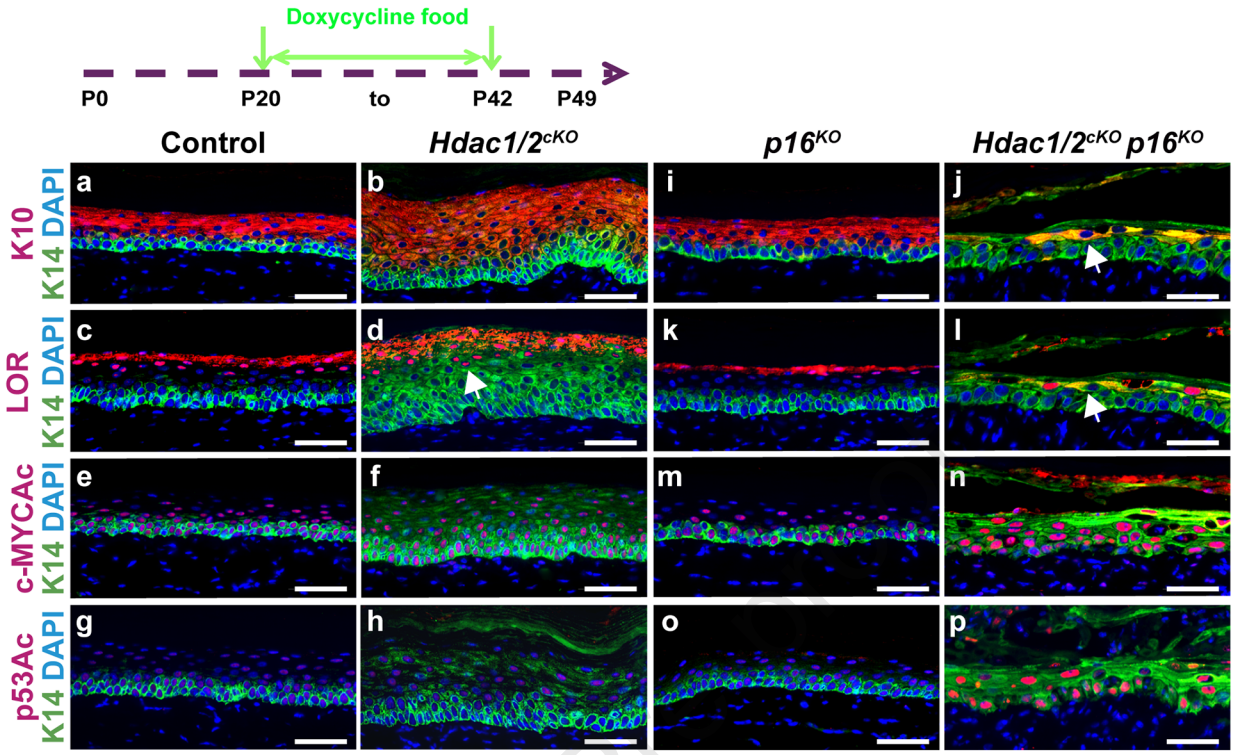
Doxycycline food
P0
P20
to
P42
P49
Control
Hdac1/2cKO
p16KO
Hdac1/2cKO p16KO
K10 K14 DAPI
LOR K14 DAPI
c-MYCAc K14 DAPI
p53Ac K14 DAPI
a
b
i
j
c
d
k
l
e
f
m
n
g
h
o
p

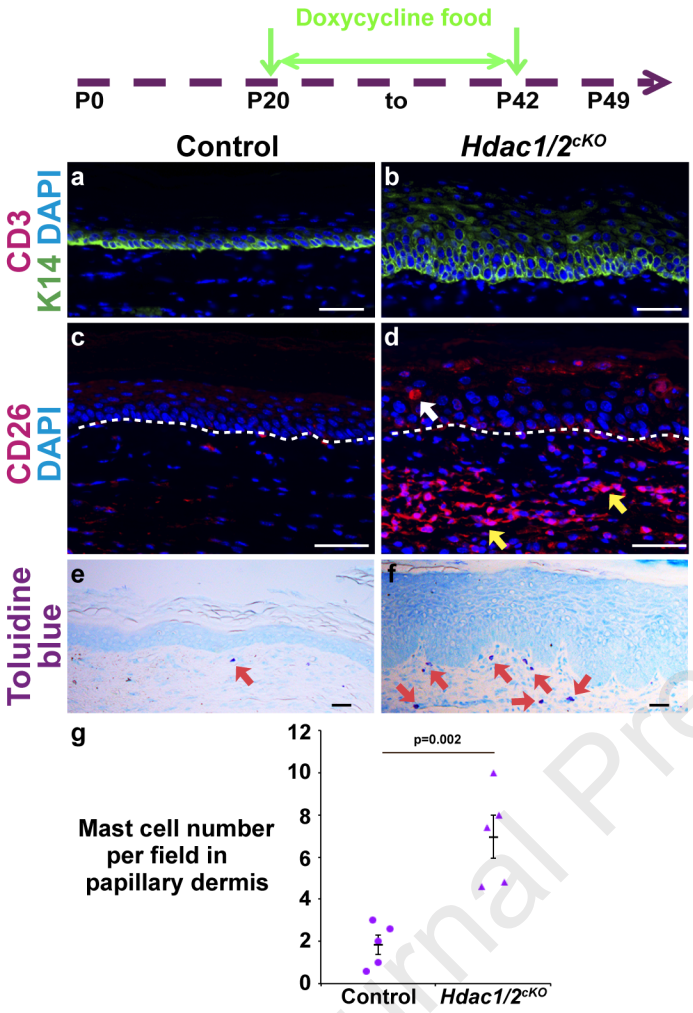

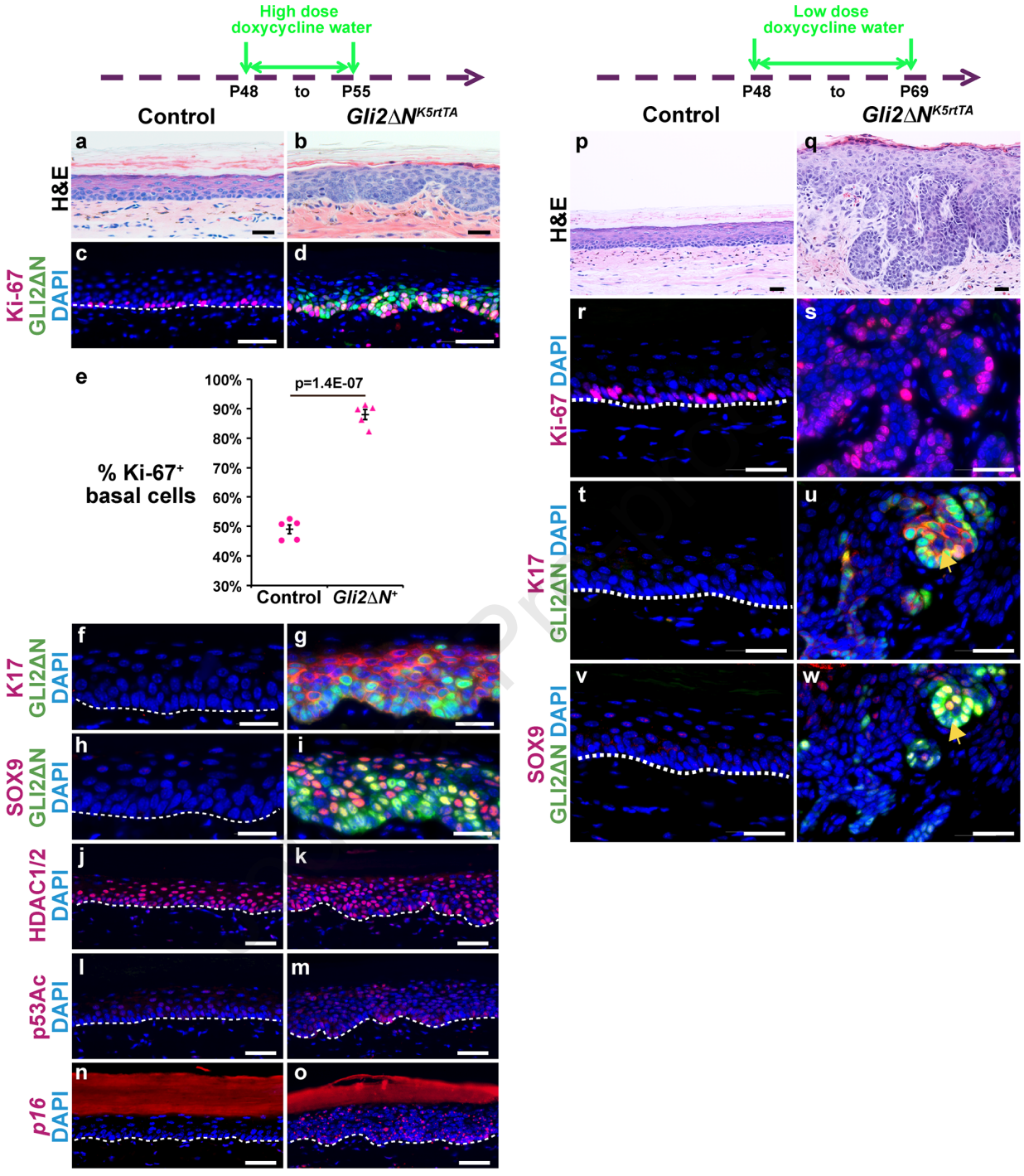
High dose
doxycycline water
P48
to
P55
Control
Gli2ΔN^K5rtTA
a
b
H&E
c
d
Ki-67
GLI2ΔN
DAPI
e
% Ki-67+
basal cells
100%
90%
80%
70%
60%
50%
40%
30%
p=1.4E-07
Control
Gli2ΔN+
f
g
K17
GLI2ΔN
DAPI
h
i
SOX9
GLI2ΔN
DAPI
j
k
HDAC1/2
DAPI
l
m
p53Ac
DAPI
n
o
p16
DAPI
Low dose
doxycycline water
P48
to
P69
Control
Gli2ΔN^K5rtTA
p
q
H&E
r
s
Ki-67
DAPI
t
u
K17
GLI2ΔN
DAPI
v
w
SOX9
GLI2ΔN
DAPI

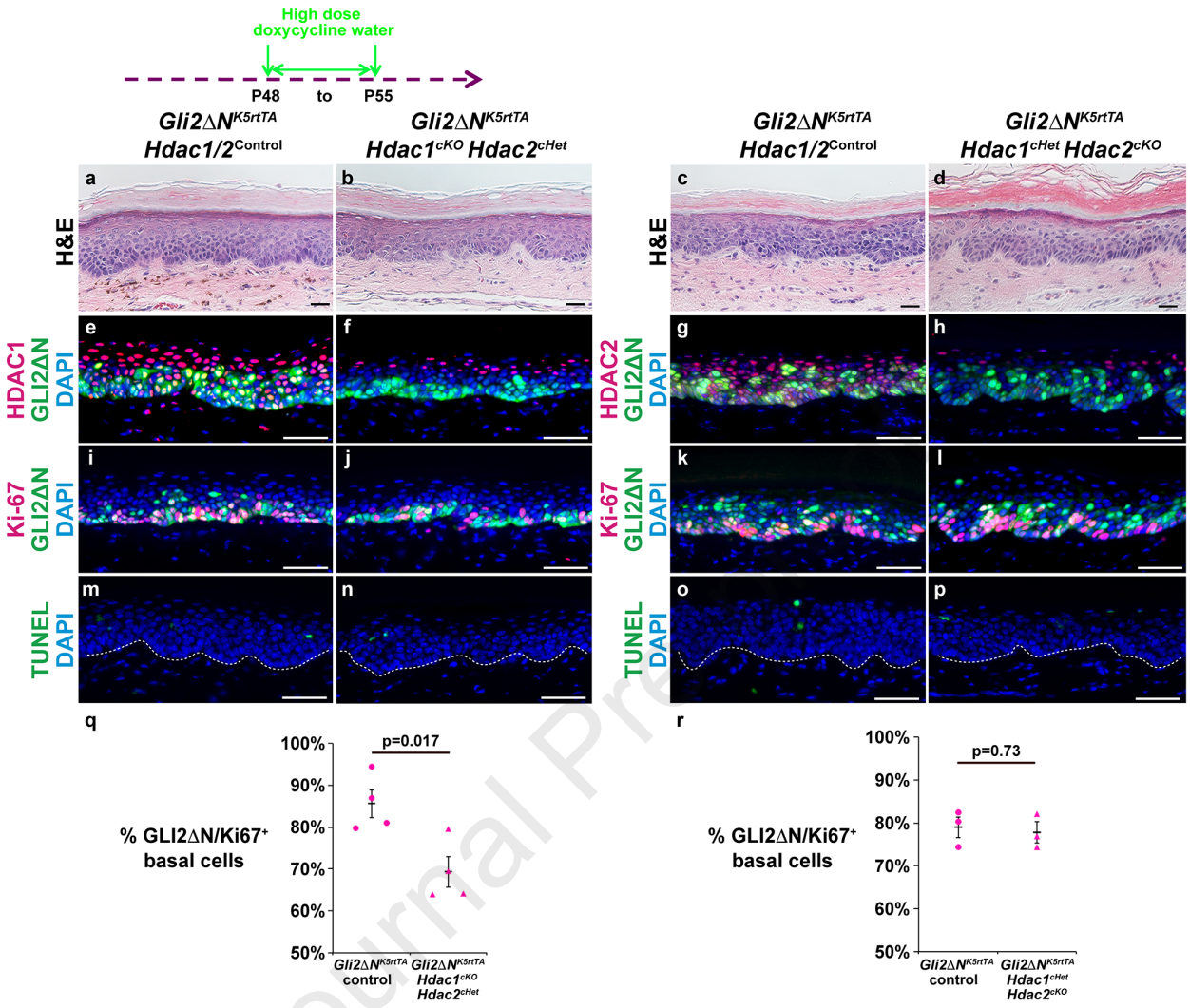
High dose
doxycycline water
P48
to
P55
Gli2ΔN K5rtTA
Hdac1/2 Control
Gli2ΔN K5rtTA
Hdac1 cKO Hdac2 cHet
Gli2ΔN K5rtTA
Hdac1/2 Control
Gli2ΔN K5rtTA
Hdac1 cHet Hdac2 cKO
H&E
HDAC1 GLI2ΔN DAPI
HDAC2 GLI2ΔN DAPI
Ki-67 GLI2ΔN DAPI
TUNEL DAPI
a
b
c
d
e
f
g
h
i
j
k
l
m
n
o
p
q
r
% GLI2ΔN/Ki67+ basal cells
100%
90%
80%
70%
60%
50%
p=0.017
p=0.73
Gli2ΔN K5rtTA control
Gli2ΔN K5rtTA Hdac1 cKO Hdac2 cHet
Gli2ΔN K5rtTA Hdac1 cHet Hdac2 cKO

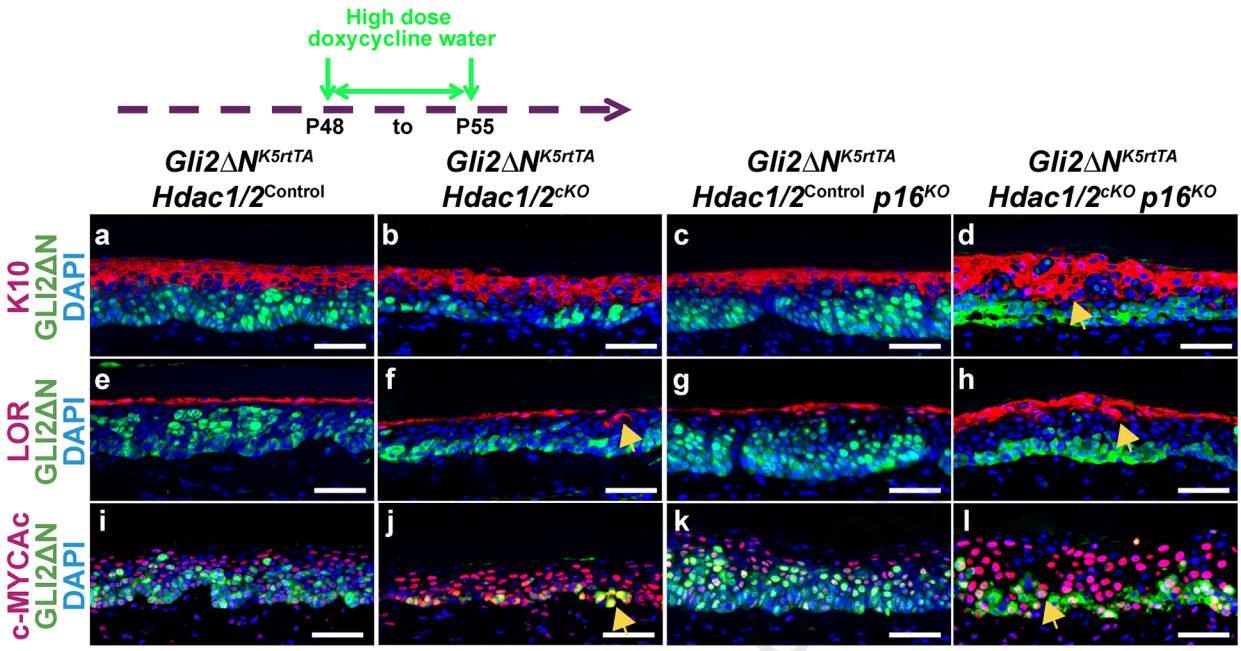

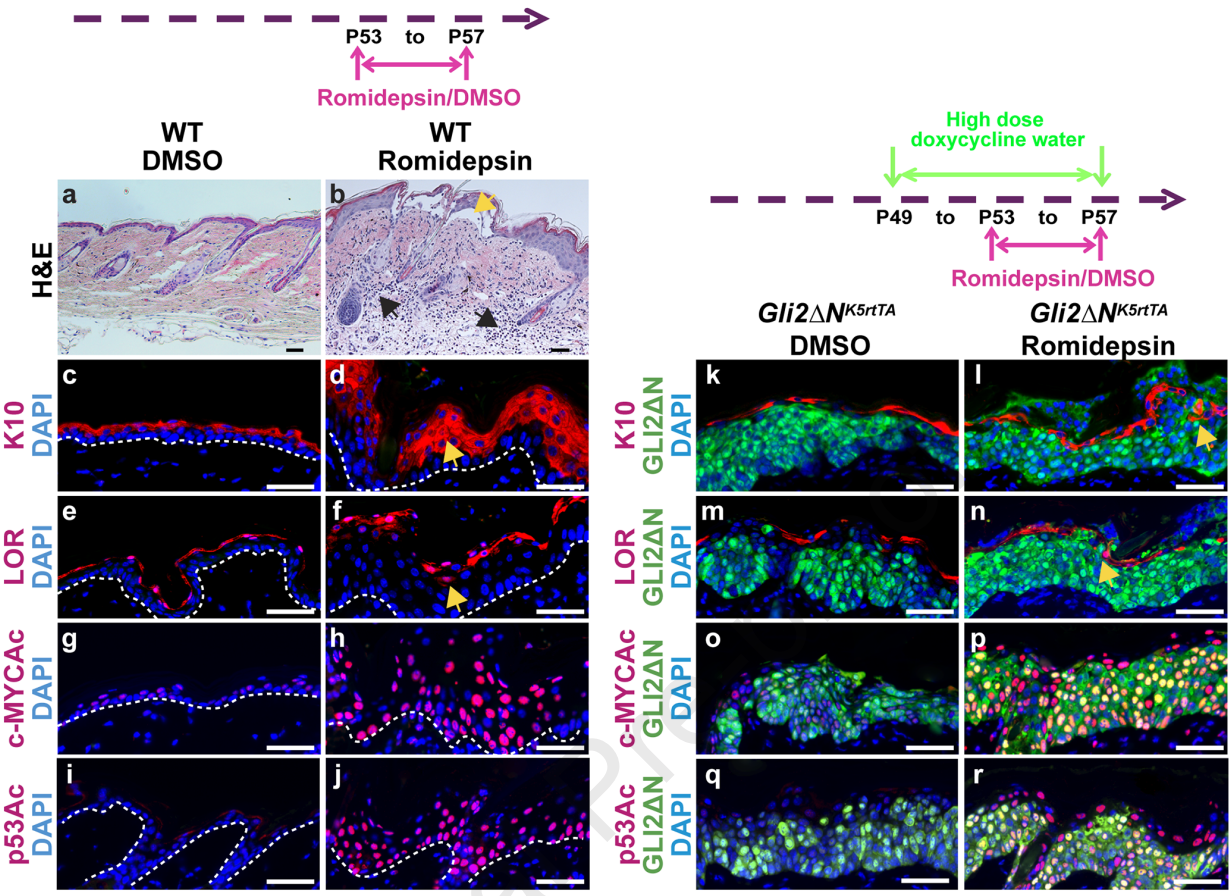
P53 to P57
Romidepsin/DMSO
WT
DMSO
WT
Romidepsin
H&E
K10
DAPI
LOR
DAPI
c-MYCAc
DAPI
p53Ac
DAPI
High dose
doxycycline water
P49 to P53 to P57
Romidepsin/DMSO
Gli2ΔN K5rtTA
DMSO
Gli2ΔN K5rtTA
Romidepsin
K10
GLI2ΔN
DAPI
LOR
GLI2ΔN
DAPI
c-MYCAc
GLI2ΔN
DAPI
p53Ac
GLI2ΔN
DAPI

HDAC1/2 control proliferation and survival in adult epidermis and pre-basal cell carcinoma via p16 and p53

Xuming Zhu, Matthew Leboeuf, Fang Liu, Marina Grachtchouk, John T. Seykora, Edward E. Morrisey, Andrzej A. Dlugosz, Sarah E. Millar

List of Supplemental Text and Figure Legends

SUPPLEMENTARY MATERIALS AND METHODS

Mice

All mice were maintained on a mixed FVB/N / C57BL/6J / SJL/J strain background. The following mouse lines were used: *Hdac1*^{fl} (Montgomery et al., 2007); *Hdac2*^{fl} (Montgomery et al., 2007); *K5-rtTA* (Diamond et al., 2000); *tetO-Cre* (Jackson Laboratories, Bar Harbor ME, strain #006234) (Perl et al., 2002); *tetO-Gli2ΔN* (Grachtchouk et al., 2011); *p53*^{KO} (Jackson Laboratories, strain #002101) (Jacks et al., 1994); and *p16*^{KO} (NCI Mouse Repository line 01XE4) (Sharpless et al., 2001). To induce Cre-mediated recombination, mice were placed on doxycycline chow (6 g/kg, Bio-Serv), or doxycycline (Sigma-Aldrich Co) containing water at high (200µg/mL in 5% sucrose) or low (10µg/mL in 5% sucrose) doses. Mice were assigned to control or experimental groups based on genotype; within each group mice were assigned randomly to experimental treatments. For most experiments we used n=5 mice per group which provides 80% power at a two-sided significance level of 0.05 to detect an effect size of 2.0s where s is the standard deviation. Mice of both sexes were analyzed and no sex-specific differences were observed in the data. All animal experiments were performed with approved animal protocols according to institutional guidelines established by the IACUC committees of the University of Pennsylvania and the Icahn School of Medicine at Mount Sinai.

Histology, immunostaining, TUNEL assays and RNAscope

Tissues dissected from euthanized mice were fixed in 4% Paraformaldehyde/PBS (Affymetrix/USB) overnight at 4 °C, and then paraffin embedded and sectioned at 5µm. Paraffin sections were de-waxed and rehydrated through xylene substitute (Sigma-Aldrich Co) and

graded ethanol solutions. Sections were microwave-treated with antigen unmasking solution (Vector Labs). For immunostaining, sections were incubated with primary antibodies overnight, followed by incubation with Alexa Fluor-labelled secondary antibodies (Thermo Fisher Scientific and Vector Labs), and application of DAPI containing mounting medium (Vector Labs). For TUNEL assays, sections were incubated with TUNEL labeling mix (Roche) at 37°C for 1 hour and then washed with PBST and mounted with DAPI containing mounting medium. RNAscope (Advanced Cell Diagnostics, Inc.) was carried out with probes for *p21* (ACD #408551), *Mdm2* (ACD #447641) and *p16* (ACD #411011) following the manufacturer's instructions.

Antibodies

The following primary antibodies were used: rabbit anti-HDAC1 (raised against the C-terminal region of human HDAC1, using a keyhole limpet haemocyanin (KLH)-conjugated synthetic peptide) (Thermo Fisher Scientific, 49-1025, 1:1000); rabbit anti-HDAC2 (raised against a synthetic 11 amino acid peptide derived from the C-terminus of the mouse HDAC2 protein) (Thermo Fisher Scientific, 51-5100, 1:1000); mouse anti-K14 (raised against a synthetic peptide corresponding to human Cytokeratin 14 (C terminal)) (Abcam, ab7800-500, 1:200); rabbit anti-acetyl-H3K9 (raised against a synthetic peptide corresponding to human Histone H3 amino acids 1-100 (N terminal) (acetyl K9) conjugated to KLH) (Abcam, ab10812, 1:500); rat anti-Ki-67 (eBioscience, 14-5698-82, 1:200); rabbit anti-K5 (raised against a peptide sequence derived from the C-terminus of the mouse keratin 5 protein) (Covance, PRB-160P, 1:1000); rabbit anti-acetyl-p53 (raised against a synthetic acetylated peptide derived from human p53 around the acetylation site of lysine 381 (Abcam, ab61241, 1:200); mouse anti-p16 (raised against amino acids 1-168

representing full length p16 of mouse origin) (Santa Cruz, sc-1661, 1:200); rabbit anti-K10 (raised against a peptide sequence derived from the C-terminus of the mouse keratin 10 protein) (Covance, PRB-159 P, 1:1,000); rabbit anti-loricrin (raised against a peptide sequence derived from the C-terminus of the mouse loricrin protein) (Covance, PRB-145 P, 1:1,000); rabbit anti-acetyl-c-MYC (raised against a KLH-conjugated linear peptide corresponding to human c-Myc acetylated at Lys157) (Millipore, ABE27, 1:200); rabbit anti-K17 (raised against a synthetic peptide within human Cytokeratin 17 amino acids 1-100 (N terminal)) (Abcam, ab109725, 1:500); rabbit anti-SOX9 (raised against a KLH-conjugated linear peptide corresponding to the C-terminal sequence of human SOX9) (Millipore, AB5535, 1:200); mouse anti-MYC-tag (raised against a synthetic peptide corresponding to residues 410-419 of human c-Myc (EQKLISEEDL)) (Cell Signaling Technology, #2276, 1:1000); rabbit anti-Ki-67 (raised against a synthetic peptide within human Ki-67 amino acids 1200-1300) (Abcam, ab16667, 1:200); rabbit anti-CD26 (raised against a synthetic peptide corresponding to Human DPP4; based on the spacer region of Human DPP4, mid-molecule, before the cysteine-rich region) (Abcam, ab28340, 1:400); rabbit anti-CD3 (raised against a synthetic peptide KAKAKPVTRGAGA corresponding to amino acids 156-168 of Human CD3 Epsilon chain) (Abcam, ab5690, 1:200).

Real-time PCR

Full thickness skin samples were incubated in Dispase II (Roche) solution for 1 hour at 37°C, and epidermis was separated from dermis with forceps. Total RNA was extracted from epidermis using TRIzol (Thermo Fisher Scientific) and purified using the RNeasy kit (Qiagen). Reverse-transcription was performed using a High-Capacity cDNA Reverse Transcription Kit (Applied Biosystems), and cDNA was subjected to real time PCR using the StepOnePlus system and

SYBR Green Kit (Applied Biosystems). *Gapdh* was used as an internal control and expression differences were determined using the $2^{-\Delta\,\Delta CT}$ method. Primers for *p16* were *p16*-Forward: 5'-GAGCATGGGTCGCAGGTTCT-3', *p16*-Reverse: 5'-GGTAGTGGGGTCCTCGCAGT-3'.

Topical application of Romidepsin

Romidepsin (Selleckchem) was diluted with DMSO to 18.5mM. Before applying to mouse skin, Romidepsin solution was diluted with corn oil to a final concentration of 0.37mM. After vigorous vortexing, 20µL Romidepsin in DMSO/corn oil or DMSO/corn oil vehicle alone was immediately applied to dorsal paw skin twice per day for four consecutive days.

Statistical Information

For quantification of Ki-67- or TUNEL-positive basal keratinocytes, basal cells were counted from five or more 20X fields per mouse. The numbers of mice used in each experiment are detailed in the figure legends. For quantification of mast cells, toluidine blue-positive dermal cells from five 20X fields were counted. For real-time qPCR, at least 3 pairs of control and mutant samples were used and 3 technical replicates were analyzed for each sample. Significance was calculated with a two-tailed Student's t-test. $P<0.05$ was considered to be significant.

SUPPLEMENTARY REFERENCES

Diamond I, Owolabi T, Marco M, Lam C, Glick A. Conditional gene expression in the epidermis of transgenic mice using the tetracycline-regulated transactivators tTA and rTA linked to the keratin 5 promoter. J Invest Dermatol 2000;115(5):788-94.

Grachtchouk M, Pero J, Yang SH, Ermilov AN, Michael LE, Wang A, et al. Basal cell carcinomas in mice arise from hair follicle stem cells and multiple epithelial progenitor populations. The Journal of clinical investigation 2011;121(5):1768-81.

Jacks T, Remington L, Williams BO, Schmitt EM, Halachmi S, Bronson RT, et al. Tumor spectrum analysis in p53-mutant mice. Current biology : CB 1994;4(1):1-7.

Montgomery RL, Davis CA, Potthoff MJ, Haberland M, Fielitz J, Qi X, et al. Histone deacetylases 1 and 2 redundantly regulate cardiac morphogenesis, growth, and contractility. Genes Dev 2007;21(14):1790-802.

Perl AK, Wert SE, Nagy A, Lobe CG, Whitsett JA. Early restriction of peripheral and proximal cell lineages during formation of the lung. Proc Natl Acad Sci U S A 2002;99(16):10482-7.

Sharpless NE, Bardeesy N, Lee KH, Carrasco D, Castrillon DH, Aguirre AJ, et al. Loss of p16Ink4a with retention of p19Arf predisposes mice to tumorigenesis. Nature 2001;413(6851):86-91.

SUPPLEMENTAL FIGURE LEGENDS

Supplemental Figure S1 – A single copy of *Hdac1* or *Hdac2* is sufficient to maintain short-term homeostasis of plantar epidermis. The schematic shows the timing of oral doxycycline treatment for panels (a-r); all samples were analyzed at P27. (a-d) Histology reveals that plantar epidermis in *Hdac1*^{cKO} *Hdac2*^{cHet} (b) and *Hdac1*^{cHet} *Hdac2*^{cKO} (d) mice is similar to controls (a,c). (e-h) IF staining for HDAC1 (e,f, red) or HDAC2 (g,h, red) shows that *Hdac1* and *Hdac2* are efficiently deleted in *Hdac1*^{cKO} *Hdac2*^{cHet} (f) and *Hdac1*^{cHet} *Hdac2*^{cKO} (h) plantar epidermis relative to their respective littermate controls. Basal cells are marked by IF for K14 (green). (i-l) IF for Ki-67 (green) shows that epidermal proliferation is similar in *Hdac1*^{cKO} *Hdac2*^{cHet} (j) and *Hdac1*^{cHet} *Hdac2*^{cKO} (l) plantar epidermis relative to their respective littermate controls (i,k). Basal cells are marked by IF for K5 (red). (m-p) TUNEL assay (green) shows that basal cell apoptosis is absent in *Hdac1*^{cKO} *Hdac2*^{cHet} (n) and *Hdac1*^{cHet} *Hdac2*^{cKO} (p) plantar epidermis and in their respective littermate controls (m,o). Epidermal-dermal borders are marked by dashed white lines. (q, r) Quantitation of the percentage of Ki-67-positive basal cells shows no statistical difference in *Hdac1*^{cKO} *Hdac2*^{cHet} (q) and *Hdac1*^{cHet} *Hdac2*^{cKO} (r) plantar epidermis relative to their respective littermate controls. Four mice of each genotype were analyzed; a two-tailed Student's *t*-test was used to calculate p-value. $p<0.05$ was considered to be significant; error bars indicate SEM. Scale bars in (a-d) and (e-p) represent 25μm and 50μm, respectively.

Supplemental Figure S2 – Loss of *p16* does not rescue proliferation or prevent apoptosis of basal cells lacking *Hdac1/2*. The schematic shows the timing of oral doxycycline treatment for panels a, c-w; samples were analyzed at P27. For panel b, mice were placed on oral doxycycline

at P19 and skin was analyzed at P28. (a) qPCR shows that *p16* mRNA expression is elevated in *K5-rtTA tetO-Cre Hdac1*$^{fl/fl}$ *Hdac2*$^{fl/fl}$ plantar epidermis relative to littermate controls. Data were normalized to *Gapdh*. Three pairs of mice were analyzed; a two-tailed Student's *t*-test was used to calculate the p-value. $p<0.05$ was considered to be significant; error bars indicate SEM. (b) Dorsal skin of *K5-rtTA tetO-Cre Hdac1*$^{fl/fl}$ *Hdac2*$^{fl/fl}$ mice doxycycline treated from P19 and analyzed at P28 shows mosaic deletion of HDAC1/2 (green) and elevated levels of p16 protein (red) in HDAC1/2 deficient cells in hair follicles (white arrow) and IFE (yellow arrow). (c-f) Histology reveals thinning of plantar epidermis in *Hdac1/2*^{cKO} (D) and *Hdac1/2*^{cKO} *p16*^{KO} (f) mice relative to control (c) and *p16*^{KO} (e) samples. (g-j) IF for HDAC1/2 (red) reveals efficient deletion in K14 positive basal cells (green) in *Hdac1/2*^{cKO} (h) and *Hdac1/2*^{cKO} *p16*^{KO} (j) plantar epidermis compared with control (g) and *p16*^{KO} (i) samples. (k-n) IF for H3K9Ac (red) reveals increased levels in *Hdac1/2*^{cKO} (l) and *Hdac1/2*^{cKO} *p16*^{KO} (n) plantar epidermis compared with control (k) and *p16*^{KO} (m) samples. IF for K14 (green) marks basal cells. (o-r) Ki-67 staining (green) reveals reduced proliferation of K5-positive basal cells (red) in *Hdac1/2*^{cKO} (p) and *Hdac1/2*^{cKO} *p16*^{KO} (r) plantar epidermis compared with control (o) and *p16*^{KO} (q) samples. (s-v) Basal cell apoptosis (green) is observed in *Hdac1/2*^{cKO} (t) and *Hdac1/2*^{cKO} *p16*^{KO} (v) plantar epidermis but not in control (s) or *p16*^{KO} (u) epidermis. (w) Quantitation of the percentage of Ki-67-positive basal cells shows that proliferation of plantar epidermis is unaltered by loss of *p16* alone compared with control; proliferation is significantly reduced in *Hdac1/2*^{cKO} epidermis and decreased proliferation is not rescued by concomitant deletion of *p16*. At least five mice of each genotype were analyzed. A two-tailed Student's *t*-test was used to calculate p-values. $p<0.05$ was considered to be significant; error bars indicate SEM. White dashed lines in (b, s-v) indicate the

boundary between epidermis and dermis. Scale bars in (b-f) and (g-v) represent 25μm and 50μm, respectively.

Supplemental Figure S3 – *p16* deletion exacerbates differentiation defects in *Hdac1/2*^{cKO} plantar epidermis after long-term doxycycline treatment. The schematic shows the timing of oral doxycycline treatment. All samples were analyzed at P42, 22 days after initiating treatment. (a, b) IF shows that expression of both K14 (green) and K10 (red) is expanded in hyperplastic *Hdac1/2*^{cKO} plantar epidermis relative to control 22 days after initiating doxycycline treatment. (c, d) IF reveals the persistence of some cells double-positive for LOR (red) and K14 (green) in hyperplastic *Hdac1/2*^{cKO} epidermis (d, white arrow) relative to control. (e, f) Levels of acetylated c-MYC (red) are similar in hyperplastic *Hdac1/2*^{cKO} epidermis and control. (g, h) Levels of p53Ac are similar in hyperplastic *Hdac1/2*^{cKO} epidermis and control. (i, j) Differentiation of *p16*-null epidermis (i), indicated by expression of K10 (red) and K14 (green) is similar to control (a). Absence of *p16* in *Hdac1/2*^{cKO} mice results in the appearance of cells strongly double-positive for K10 and K14 (j, arrow; compare with b). (k, l) Differentiation of *p16*-null epidermis (k), indicated by expression of LOR (red) and K14 (green) is similar to control (c). Absence of *p16* in *Hdac1/2*^{cKO} mice results in the appearance of cells strongly double-positive for LOR and K14 (l, arrow; compare with d). (m, n) Cells with high levels of acetylated c-MYC (red) are retained in *Hdac1/2*^{cKO} *p16*^{KO} triple-mutant epidermis after 22 days of doxycycline treatment (n), but are absent in *p16*^{KO} epidermis (m), control epidermis (e) and repopulated *Hdac1/2*^{cKO} epidermis (f). (o, p) Cells with high levels of acetylated p53 are retained in *Hdac1/2*^{cKO} *p16*^{KO} triple mutant epidermis after long-term doxycycline induction (p) but are absent in *p16*^{KO} epidermis (o),

control epidermis (g) and repopulated *Hdac1/2*^{cKO} epidermis (h). At least four mice of each genotype were analyzed in each experiment. Scale bars represent 50μm.

Supplemental Figure S4 – *Hdac1/2*^{cKO} skin displays inflammation 22 days after initiating deletion. (a-f) At 22 days after initiating doxycycline treatment, *Hdac1/2*^{cKO} plantar skin displays thickening of the epidermis relative to control. $CD3^+$ T-cells are absent in control and mutant skin (a,b); however, expression of the inflammatory marker CD26 is elevated in mutant epidermis and dermal fibroblasts relative to control (c,d; red signal, arrows) and mutant dermis displays increased numbers of mast cells (e,f; purple signal, arrows). Dashed lines represent epidermal-dermal borders. Scale bars represent 50μm (a-d) or 30μm (e,f). (g) Quantitation of mast cell numbers shows that these are significantly increased in *Hdac1/2*^{cKO} plantar skin relative to controls 22 days after initiating doxycycline treatment. 5 pairs of mutant and control mice were analyzed. A two-tailed Student's *t*-test was used to calculate the p-value. $p<0.05$ was considered to be significant; error bars indicate SEM.

Supplemental Figure S5 – Forced expression of GLI2ΔN in plantar epidermis initiates BCC-like tumorigenesis. The left schematic indicates the timing of treatment with high-dose doxycycline water in panels (a-i); samples were analyzed at P55, 7 days after initiating treatment. The right schematic indicates the timing of treatment with low-dose doxycycline water in panels (j-q); samples were analyzed at P69, 21 days after initiating treatment. (a, b) Histology shows thickening and invagination of plantar epidermis 7 days after initiating high-dose doxycycline treatment to induce expression of GLI2ΔN (b) compared with littermate control (a). (c, d) IF shows efficient induction of expression of GLI2ΔN (green) and increased proliferation (red) in

K5-rtTA tetO-GLI2ΔN epidermis (d) compared with control (c). (e) Quantitation of the percentage of Ki-67-positive basal cells shows that proliferation is significantly increased in induced *K5-rtTA tetO-GLI2ΔN* epidermis compared with control. Five pairs of control and mutant mice were analyzed. A two-tailed Student's *t*-test was used to calculate p-value. $p<0.05$ was considered significant; error bars indicate SEM. (f-i) GLI2ΔN-expressing plantar epidermis shows ectopic expression of BCC markers K17 (red) (f,g) and SOX9 (red) (h,i). (j-m) HDAC1/2 protein levels are unchanged and acetylated p53 is slightly elevated in GLI2ΔN-expressing plantar epidermis. (n,o) RNAscope shows slightly elevated levels of p16 mRNA in GLI2ΔN-expressing plantar epidermis. (p,q) Histology shows that long-term induction with low dose doxycycline water results in tumor development resembling human superficial BCC. (r,s) Lesions resulting from long-term induction of *K5-rtTA tetO-GLI2ΔN* mice show robust proliferation at the leading edges of the downgrowths, as indicated by Ki-67 staining (red). (t-w) Lesions resulting from long-term induction of *K5-rtTA tetO-GLI2ΔN* mice express the BCC markers K17 (red) (t,u) and SOX9 (red) (v,w) (arrows in u,w). IF for myc-tagged GLI2ΔN is shown in green. Five pairs of GLI2ΔN-expressing and control mice were analyzed in (a-o); two pairs of GLI2ΔN-expressing and control mice were analyzed in (p-w). Control mice lacked *K5-rtTA* or *tetO-GLI2ΔN* transgenes. Scale bars represent 25μm in (a,b,f-i,p,q), 50μm in (c,d; j-o), and 30μm in (r-w).

Supplemental Figure S6 - HDAC1 and HDAC2 act semi-redundantly in regulating pre-BCC development. The schematic shows the timing of treatment with high-dose doxycycline water; all samples were analyzed at P55 after 7 days of treatment. (a-d) Histology shows that homozygous loss of *Hdac1* combined with heterozygous loss of *Hdac2* (b) or heterozygous loss

of *Hdac1* combined with homozygous loss of *Hdac2* (d) has no obvious effect on the morphology of GLI2ΔN-driven pre-BCC in plantar epidermis compared with controls (a,c). (e-h) IF for GLI2ΔN (green) and HDAC1 (e,f, red) or HDAC2 (g,h, red) shows that *Hdac1* or *Hdac2* are efficiently deleted in GLI2ΔN-expressing basal cells in mice carrying homozygous $Hdac1^{cKO}$ or homozygous $Hdac2^{cKO}$ alleles, respectively. (i-l) IF for GLI2ΔN (green) and Ki-67 (red) shows that homozygous loss of *Hdac1* combined with heterozygous *Hdac2* deletion (j) reduces proliferation compared with the littermate control (i) whereas heterozygous loss of *Hdac1* combined with homozygous *Hdac2* deletion (l) does not affect proliferation compared with control (k). (m-p) TUNEL assay (green) shows that basal cell apoptosis is absent in GLI2ΔN-expressing epidermis with homozygous loss of *Hdac1* combined with heterozygous *Hdac2* deletion (n) or heterozygous loss of *Hdac1* combined with homozygous *Hdac2* deletion (p) as well as in littermate controls (m,o). (q,r) Quantitation of the percentage of GLI2ΔN-expressing basal cells positive for Ki67 shows a significant decrease in proliferation in epidermis with homozygous loss of *Hdac1* combined with heterozygous *Hdac2* deletion (q) but no significant change in proliferation in epidermis with heterozygous loss of *Hdac1* combined with homozygous *Hdac2* deletion (r). Four pairs of control and mutant mice were analyzed in (q); three pairs of control and mutant mice were analyzed in (r). A two-tailed Student's *t*-test was used to calculate p-values. $p<0.05$ was considered significant; error bars indicate SEM. Scale bars represent 25μm in (a-d) and 50μm in (e-p).

Supplemental Figure S7 - Loss of *p16* exacerbates abnormal differentiation in *Hdac1/2*-deficient GLI2ΔN-expressing plantar epidermis. The schematic shows the timing of treatment with high-dose doxycycline water; plantar epidermis was analyzed at P55 after 7 days of

treatment. (a-d) IF for GLI2ΔN (green) and K10 (red) shows that K10 expression is slightly expanded in *Hdac1/2* deleted GLI2ΔN-expressing epidermis (b) compared with GLI2ΔN-expressing control (a); deletion of *p16* alone does not alter K10 expression in GLI2ΔN-expressing epidermis (c, compare with a); co-deletion of *p16* and *Hdac1/2* enhances expansion of K10 expression (d, arrow) compared with *Hdac1/2* deletion alone (b). (e-h) IF for GLI2ΔN (green) and LOR (red) shows that LOR expression is slightly expanded in *Hdac1/2* deleted GLI2ΔN-expressing epidermis (f, arrow) compared with GLI2ΔN-expressing control (e); deletion of *p16* alone does not alter LOR expression in GLI2ΔN-expressing epidermis (g, compare with e); co-deletion of *p16* and *Hdac1/2* enhances expansion of LOR expression (h, arrow) compared with *Hdac1/2* deletion alone (f). (i-l) IF for GLI2ΔN (green) and acetylated c-MYC (red) shows that acetylated c-MYC levels are higher in *Hdac1/2* deleted GLI2ΔN-expressing epidermis (j, arrow) compared with GLI2ΔN-expressing control (i); deletion of *p16* alone does not alter acetylated c-MYC levels in GLI2ΔN-expressing epidermis (k, compare with l); co-deletion of *p16* and *Hdac1/2* appears to further enhance levels of acetylated c-MYC (l, arrow) compared with *Hdac1/2* deletion alone (j, arrow). 5 mice of each genotype were analyzed. Scale bars represent 50μm.

Supplemental Figure S8 – Topical Romidepsin causes abnormal differentiation of normal and GLI2ΔN-expressing IFE. The schematics indicate the timeframes for treatment of dorsal paw skin with topical Romidepsin or vehicle, and oral high-dose doxycycline water; all samples were analyzed at P57. (a,b) Romidepsin-treated dorsal paw skin exhibits epidermal damage (yellow arrow), abnormal hair follicles, and the presence of an inflammatory infiltrate in the dermis (black arrows). (c-j) Romidepsin-treated dorsal paw IFE (d,f,h,j) displays expanded K10

(red) (d) and LOR (red) (f) expression (yellow arrows), and increased levels of acetylated c-MYC (red) (h) and acetylated P53 (red) (j), compared with vehicle-treated IFE (c,e,g,i). White dashed lines indicate epidermal-dermal borders. (k-r) Romidepsin-treated GLI2ΔN-expressing dorsal IFE displays slightly expanded K10 (red) (l) and LOR (red) (n) expression (yellow arrows), and increased levels of acetylated c-MYC (red) (p) and acetylated P53 (red) (r), compared with vehicle-treated GLI2ΔN-expressing IFE (k,m,o,q). IF for myc-tagged GLI2ΔN is shown in green. n=5 vehicle-treated and 5 Romidepsin-treated mice in (a-j); n=4 vehicle-treated and 4 Romidepsin-treated mice in (k-r). Scale bars represent 50μm.